

# Mathematical Modelling and Numerical Simulation of Maisotsenko Cycle

Rasikh Tariq, Fatima Z. Benarab

**Abstract**— Evaporative coolers has a minimum potential to reach the wet-bulb temperature of intake air which is not enough to handle a large cooling load; therefore, it is not a feasible option to overcome cooling requirement of a building. The invention of Maisotsenko (M) cycle has led evaporative cooling technology to reach the sub-wet-bulb temperature of the intake air; therefore, it brings an innovation in evaporative cooling techniques. In this work, we developed a mathematical model of the Maisotsenko based air cooler by applying energy and mass balance laws on different air channels. The governing ordinary differential equations are discretized and simulated on MATLAB. The temperature and the humidity plots are shown in the simulation results. A parametric study is conducted by varying working air inlet conditions (temperature and humidity), inlet air velocity, geometric parameters and water temperature. The influence of these aforementioned parameters on the cooling effectiveness of the HMX is reported. Results have shown that the effectiveness of the M-Cycle is increased by increasing the ambient temperature and decreasing absolute humidity. An air velocity of 0.5 m/sec and a channel height of 6-8mm is recommended.

**Keywords**—Renewable energy, indirect evaporative cooling, Maisotsenko cycle, HMX, mathematical model, numerical simulation.

## I. INTRODUCTION

AIR conditioning becomes one of the crucial comforts of life needs. The demand of energy to cool the building envelope have raised significantly in the world as it accounts roughly for 40% of building energy consumption across the world [1]. Heating, Ventilation and Air Conditioning (HVAC) systems are the major energy consumers in a building which is around 50% of the total supplied energy [2]. Vapor Compression Refrigeration Cycle (VCRC) takes heat from the room by evaporating the refrigerant in the evaporator and rejects it in the environment through condenser. Recent observation lead to the fact that VCRC is not the long lasting solution of space cooling [3]. The highlight of this weaknesses are basically: the high initial capital cost, refrigerants have a potential of ozone depletion, global warming, and compressors are energy inefficient, thus, consumes a lot of electricity i.e. high running cost. The COP of VCRC decreases as the outside temperature of environment increases because the compressor has to work more to reject heat in the environment for the same tons of refrigeration. This situation has raised concerns over depletion of energy resources and contributing to global warming [3], which would push back to the purchase of air

conditioners and so on. These effects of air conditioning are seen as an environmental bomb. This pushes the idea of using the renewable energy for air conditioning. Renewable solutions are available for space cooling like: solar cooling, which use the heat of sun for cooling air, Geothermal technology, bioenergy technologies [4] and EC. The major concern of this work is about EC.

EC system uses the latent heat of water for cooling purposes. EC systems are renewable to environment since they do not use any harmful refrigerant instead they just use water and air for cooling purposes [5]. Although EC systems consume less electricity and they are environment-friendly but still they lack a technical barrier of handling a large sensible cooling load. Moreover, the evaporative coolers are mainly dependent on the relative humidity of the environmental air. EC has three types:

### A. Direct Evaporative Cooling (DEC)

In DEC, dry hot air passes through the wet channel causing water evaporation. Since evaporation needs energy, so the air cools down to its WB temperature. During the water evaporation, the absolute humidity of air increases because mass transfer occurs from water to air because of concentration gradient, and as a result high humidity level causes discomfort for occupants

### B. Indirect Evaporative Cooling (IEC)

In an IEC the air is divided into two parts: working air and product air.

The product air is supplied to the room. Working air passes through wet channel and product air passes through dry channel. Working air in wet channel causes evaporation and it reaches its WB temperature. The same working air is used to cool the product air. Since, the product air is not in any direct contact with water so, its absolute humidity remains unchanged. The results of the research show that WB effectiveness of IEC (60-80%) is less than DEC (90-100%)[6].

### C. Modifications in an IEC – The M Cycle

M-Cycle is a structural modification of an IEC method [7]. Using M-Cycle air can be cooled to a temperature below its WB and above its dew point temperature. Fig. 1 is the schematic of HMX. The two air channels are shown in Fig. 1. The working air takes hot and dry air from the environment, first it passes through the dry channel, and then it passes through the wet channel.

R. T. is with Department of Mechanical Engineering, HITEC University, Taxila, 47080 Pakistan (e-mail: rasikh.tariq@hitecuni.edu.pk).

F. Z. B is with Laboratory of Mechanics, University Amar Telidji Laghouat, 03000 Algeria (e-mail: f.benarab@lagh-univ.dz).

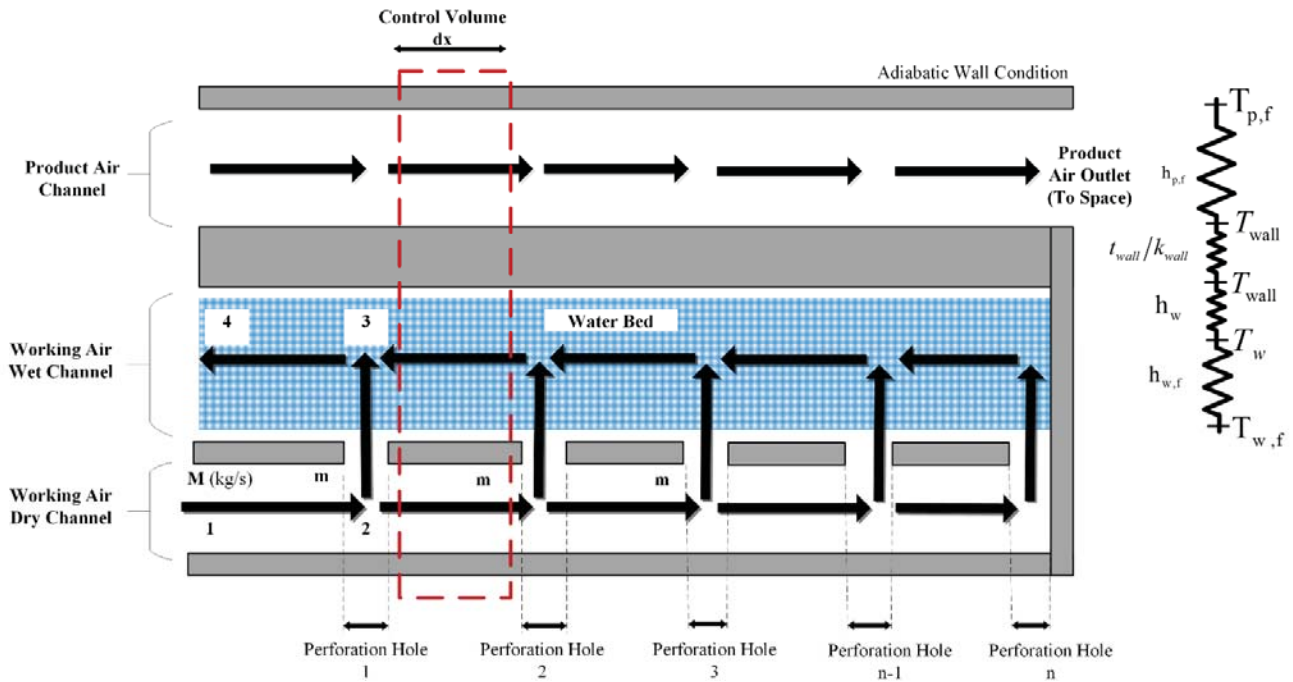


Fig. 1 Schematic of HMX along with control volume

According to M-Cycle principle, the product air can be cooled below its WB temperature and above its dew point temperature unlike IEC in which the air can't even reach its WB temperature. Fig. 2 shows the process on a psychrometric chart. Working Air is used to cool the product air. It enters the HMX and acts as a refrigerant. The working air cools down a bit (Process 1-2 of Fig. 2), without any increase of absolute humidity. The process can be modelled as "**Sensible Cooling**". The working air cools down because of the evaporation happening in wet channel of working air. Then, a portion of working air "m" is diverted towards the wet channel through a perforation hole. Now, this air gives its energy to evaporate water. Since, the working air gives its energy for water evaporation, so it cools down. It cools down further and reaches its saturation temperature where its relative humidity RH is 100%, because of presence of water. This process can be modelled as "**Cooling and Humidification**" and is shown as 2-3 in Fig. 2.

Now, this working air is capable to absorb heat from the product air, and remaining working air in dry working channel. It heats up because it is absorbing enthalpy, and leaves the HMX keeping its 100% relative humidity saturation. This process is modelled as "**Enthalpy Addition at 100% RH**" and is shown as 3-4 in Fig. 2.

The process repeats itself until product air reaches below the WB temperature. The psychrometric chart of all these processes is shown in Fig. 2.

The mathematical model of this HMX process yields coupled differential equations. Several researches have been done in the analytical and numerical models of solving coupled Heat and mass transfer ordinary differential equations (ODE) of HMX. However, it still needs some development and improvement. Yi Jiang, & Xiaoyun Xie [5], presented a theoretical analysis and

practical performance of a novel indirect-evaporative chiller. This tested indirect-evaporative chiller reaches a COP of 9.1 thus it can save more than 40% energy than the conventional water-chillers. Hakan [8] et al, did the thermodynamic performance assessment by applying energy & exergy analysis on M-Cycle. Exergy analysis was carried out for six reference temperatures and specific flow exergy, exergy input, exergy output, exergy destruction, entropy generation rates etc were determined for each case and concluded that optimum operation occurs a reference temperature of 23.88°C, a prototype was built up and experimentally investigated with integrated liquid desiccant. X. Cui et al. [9] presented an analytical model for indirect- EC heat exchanger using modified log-mean-temperature-difference (LMTD) method which was originally used for sensible heat exchangers. Their method shows ±8% of uncertainty with experimental methods. After that they also worked on counter-flow indirect-evaporative cooler HMX using Eulerian-Lagrangian CFD model [10]. Zhao et al. [11] analysed the novel M-Cycle unit with the counter flow arrangement. They showed that product air can be cooled below its WB temperature using their structural modification in an IEC. They also suggested several design conditions, which allow obtaining higher cooling effectiveness. Gao et al. [12] presented a model consists of two air-handling systems: the moisture removal using desiccant and sensible heat removal using M-Cycle, whereas the performance of moisture removing stage affects the performance of the other stage. They also worked on M-cycle IEC. [13] and observed changes in temperature and humidity plots of air and desiccant solution, and they concluded that changing initial parameters effect the performance of HMX. Sergey Anisimov and Demis Pandelidis [14] presented a numerical modelling of M-Cycle using modified ε-NTU method and quantified overall heat exchanger

performance. M. Jradi and S. Riffat [15] proposed a numerical study by modifying the HMX resulting a temperature below the air wet-bulb temperature and towards its dew point temperature. The model was simulated and they predicted the air-temperature and humidity distributions.

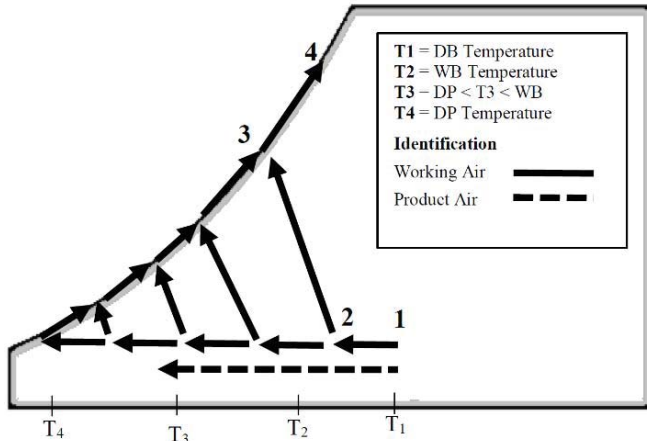


Fig. 2 Psychrometric chart of M Cycle processes

Demis Pandelidis [16], [17] did analysis of selected configurations of M Cycle based HMX s and their cooling performance is predicted [18]. Their analysis is originally based on the modified  $\epsilon$ -NTU method.

In their recent work Pandelidis [19] did a numerical analysis of the desiccant system equipped with the cross-flow M-Cycle indirect evaporative air cooler. The study was performed with the assumption of relatively low temperature of the desiccant wheel regeneration airflow, which can be obtained using solar energy in moderate climate conditions. The results indicated that the novel system allows for higher temperature effectiveness than the traditional solution even when the desiccant wheel is regenerated with lower temperature. The additional advantage of the M-Cycle exchanger is that it does not add moisture to the airflow, which allows providing more comfort to the conditioned spaces. O. Khalid [20] established an experimental setup of an EC system based on M-Cycle. The focus of the research is design and development of cost effective small scale air conditioning unit. Experimental study targets low air flow rates and the results of the purposed design shown that the WB effectiveness ranged between 92 and 20%, whereas the dew point effectiveness varied between 62 and 85% for various inlet conditions.

## II. MATHEMATICAL MODEL

The mathematical model of M-Cycle is formulated by applying heat and mass balance equations on the dry and wet channels of the HMX having a counter flow arrangement. Fig. 1 shows the channels of HMX along with their thermal circuits. The wet channels contain a wicking material and is saturated with water. It is considered that the mass flow rate of water is small, therefore, is considered as stagnant film. Hydrodynamic entry length and thermal entry length are small as compared to channel length, therefore, is neglected in proposed

mathematical model. The heat and mass transfer process in HMX is considered adiabatic and steady state. Momentum and thermal properties are taken as uniform for selected control volume. The preceding assumptions have shown insignificant effect on temperature and humidity plots in both channels [6], [21].

A product mass flow rate ( $m_{p,f}$ ) with specific heat ( $c_{p,f}$ ) enters the product air channel of cross sectional area ( $A_d$ ) having the length of channel ( $L_d$ ), the temperature of the interface ( $T_s$ ) between the working air and the water film is assumed to be equal to the water temperature ( $T_w$ ), therefore, on the dry side of product air channel, the sensible heat transfer equation is written for a differential control volume ( $dx$ ):

$$\frac{dT_{p,f}}{dx} = \frac{k_{p,f} A_d}{L_d m_{p,f} c_{p,f}} (T_w - T_{p,f}) \quad (1)$$

The overall heat transfer coefficient  $k_{p,f}$  is defined as:

$$k_{p,f} = \frac{1}{\frac{1}{h_{p,f}} + \frac{t_{wall}}{k_{wall}} + \frac{1}{h_w}}$$

It is assumed that the water is film is static; therefore, the convection coefficient of water is zero i.e.  $h_w = 0$ . The thickness of the wall ( $t_{wall}$ ) is small, whereas it's thermal conductivity ( $k_{wall}$ ) is high. As a result, the ratio  $\frac{t_{wall}}{k_{wall}}$  approaches to zero.

Equation (2) is the product air temperature distribution equation.

$$\frac{dT_{p,f}}{dx} = \frac{h_{p,f} A_d}{L_d m_{p,f} c_{p,f}} (T_w - T_{p,f}) \quad (2)$$

The wet side involves both the heat and mass transfer between the working air wet channel and working air dry channel, product air and water. The mass balance equation applied between the working air wet channel and water film yields humidity distribution ( $\omega_{w,f}$ ) equation as:

$$\frac{d\omega_{w,f}}{dx} = \frac{h_m A_w}{L_w \dot{m}_{w,f}} (\omega_{w,s} - \omega_{w,f}) \quad (3)$$

whereas,  $\omega_{w,s}$  is the saturated absolute humidity at 100% relative humidity at working air temperature ( $T_{w,f}$ ). Energy balance on working air wet channel yields its temperature plot equation, as:

$$\frac{dT_{w,f}}{dx} = \left[ \frac{h_{w,f} A_w}{c_{p,m} L_w \dot{m}_{w,f}} (T_w - T_{w,f}) + \frac{c_{p,v} d\omega_{w,f}}{c_{p,m} dx} (T_w - T_{w,f}) \right] \quad (4)$$

whereas, the specific heat of moist air ( $c_{p,m}$ ) is calculated using specific heat of dry air ( $c_{p,a}$ ) and specific heat of vapor ( $c_{p,v}$ ) using equation  $c_{p,m} = c_{p,a} + \omega_{w,f} c_{p,v}$ . Considering a surface wettability factor of 1, an overall heat balance on the entire HMX yields the equation:

$$\frac{dT_w}{dx} = \frac{A}{m_w L} \left[ \frac{h_{hf}}{c_{pw}} (T_w - T_{hf}) + \frac{h_{wf}}{c_{pw}} (T_w - T_{wf}) + h_m \left( \frac{c_{pw}}{c_{pw}} + \frac{i_o}{c_{pw}} - T_w \right) (\omega_{ws} - \omega_{wf}) \right] \quad (5)$$

The Reynolds Number is defined as:

$$Re = \frac{\rho v D_h}{\mu}$$

$D_h$  is the hydraulic diameter and calculated using:  $D_h = \frac{4A_{cross}}{P}$ . The convective heat transfer coefficient is calculated using Nusselt Number as:  $h = \frac{Nu \times k}{l}$ . Sieder and Tate correlation [22] is used to evaluate Nusselt Number which is:

$$Nu = 1.86 \left( \frac{RePr}{L/D_h} \right)^{\frac{1}{3}} \left( \frac{\mu}{\mu_s} \right)^{0.14} \quad (6)$$

The working air side convective mass transfer coefficient is computed using Sherwood Number which is calculated using the correlation [23]:

$$Sh = 0.023 Re^{0.83} Sc^{1/3} \quad (7)$$

The Schmidt Number ( $Sc$ ) is calculated using dynamic viscosity and mass diffusivity ( $D$ ). The mass diffusivity is a constant in Ficks law and is calculated using the following empirical relationship [24]. Valid for only water and air:

$$D = 21.2 \times 10^{-6} (1 + 0.0071 T_{w,f})$$

The WB ( $\epsilon_{w,b}$ ) and dew point effectiveness ( $\epsilon_{dp}$ ) is calculated using DB temperature of working air ( $T_{DBw,f,in}$ ), DB temperature of product air ( $T_{DBp,f,out}$ ), WB temperature of working air ( $T_{WBw,f,in}$ ), and dew point temperature of working air ( $T_{DPw,f,in}$ ) as:

$$\epsilon_{w,b} = \frac{T_{DBw,f,in} - T_{DBp,f,out}}{T_{DBw,f,in} - T_{WBw,f,in}} \quad (8)$$

$$\epsilon_{dp} = \frac{T_{DBw,f,in} - T_{DBp,f,out}}{T_{DBw,f,in} - T_{DPw,f,in}} \quad (9)$$

It should be stressed that the WB and the dew point effectiveness are the major parameters to evaluate the performance of HMX, as these parameters measure the extent to which the product air can be cooled.

### III. METHODOLOGY

The governing ordinary differential coupled heat and mass transfer equations with coupled boundary equations are discretized using first order forward direction finite difference scheme. MATLAB 2014a, The MathWorks, Natick, 2014 is used to simulate M-Cycle processes. The iteration steps and methodology is shown in Fig. 3.

Suitable numbers of elements i.e. 1500 are selected for iteration purpose depending on the compromise between accuracy and computational speed as shown in Fig. 4.

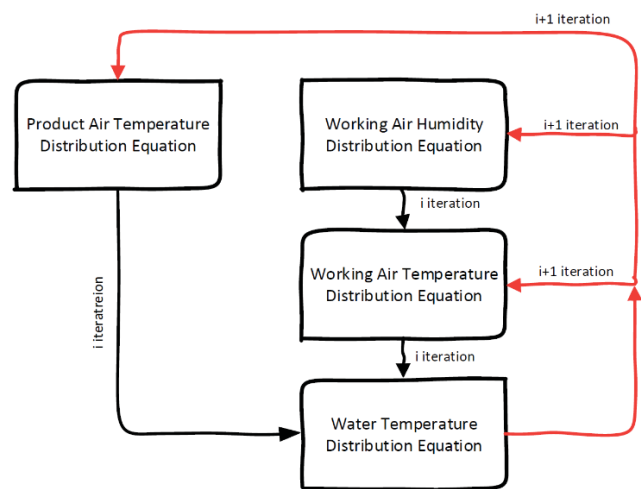


Fig. 3 Methodology Diagram

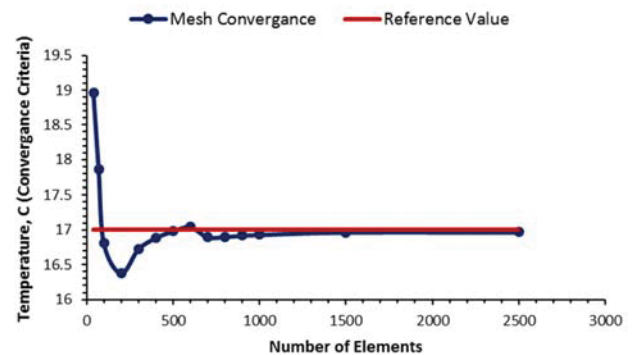


Fig. 4 Convergence Criteria

Table I shows the geometrical parameters and operating conditions in addition with operational conditions of HMX.

### IV. VALIDATION OF RESULTS

The model is validated using the experimental results of a counter flow dew point EC based heat exchanger developed by Rianguviku and Kumar [6]. Rianguviku and Kumar [6] carried out experiments to investigate product air outlet conditions and HMX effectiveness at different working air inlet



conditions. The experimental conditions of [6] are precisely replicated in the current Matlab simulation. The presented model is validated by comparing the outlet working wet channel air conditions with of [6] as presented in Fig. 5. It can be observed that the discrepancy in compliance of simulated and experimental data is  $\pm 10\%$ .

TABLE I:  
 OPERATING CONDITIONS AND GEOMETRIC PARAMETERS OF HMX

| Symbol | Parameter                  | Quantity |
|--------|----------------------------|----------|
| $L_d$  | Length of Dry Channel      | 720 mm   |
| $L_w$  | Length of Wet Channel      | 720 mm   |
| -      | Width of Channel           | 25 mm    |
| -      | Channel Height             | 4 mm     |
| $T_w$  | Supply Water Temperature   | 17°C     |
| -      | Product Air Inlet Velocity | 1 m/sec  |
| -      | Working Air Inlet Velocity | 1 m/sec  |

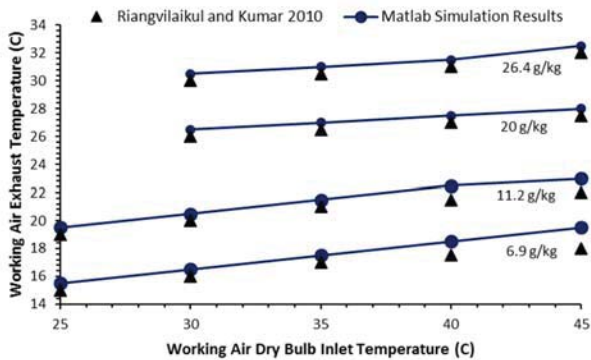


Fig. 5 Validation of the Simulation Results by comparison with Rianguvikaal and Kumar [6]

## V. RESULTS AND DISCUSSION

Simulation is carried out to investigate the performance of HMX on different operating conditions.

### A. Temperature & Humidity Plots

Temperature and humidity plots of product air, working air dry channel, and working air wet channel is shown in Fig. 6-8.

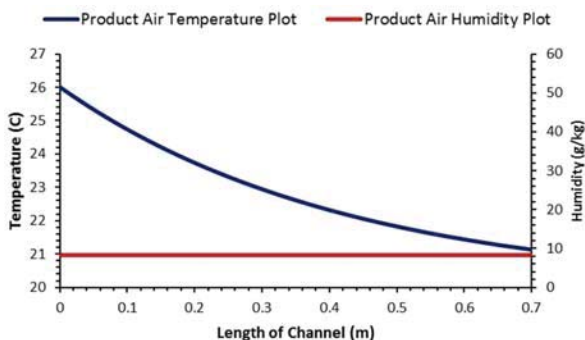


Fig. 6 Product Air Temperature & Humidity Plot

The inlet working air dry channel temperature is taken as 40°C and 11g/kg of absolute humidity which are normal atmospheric conditions for a dry and hot location.

The WB temperature of working air is 23.5°C and a dew

point temperature of 15°C. It can be observed in Fig. 6 the product air outlet temperature is around 21°C which is a temperature between WB and dew point of inlet working air temperature; however, its humidity remains unchanged. The same phenomena can be observed in Fig. 2 where product air is cooled below the WB temperature of working air. Fig. 7 shows the temperature and humidity plot of working air-dry channel. It can be observed that working air in dry channel undergoes no humidity change because there is no contact with water in working air dry channel. The humidity and temperature of working air wet channel increases while moving towards the exhaust of HMX because it absorbs heat content from remaining working air and product air, and moisture content by water evaporation as depicted in Fig. 8. A similar pattern of humidity and temperature distribution is also simulated by Zhao et al. [11] and Jradi et al. [15].

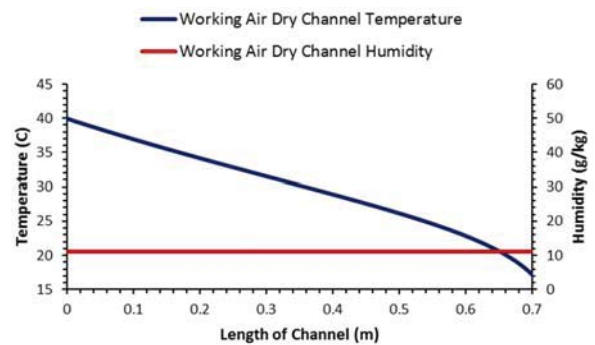


Fig. 7 Working Air-Dry Channel Temperature & Humidity Plot

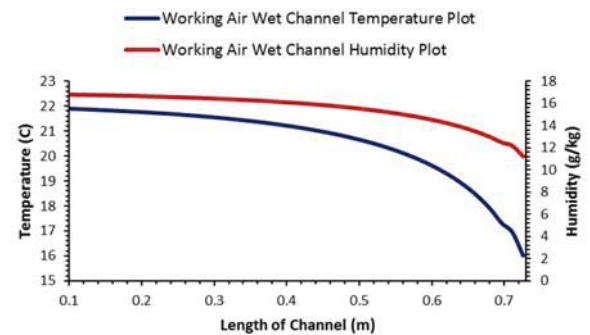


Fig. 8 Working Air Wet Channel Temperature & Humidity Plot

### B. Effect of Working Air Inlet Conditions (Temperature & Humidity) on Cooling Effectiveness

The WB and dew point cooling effectiveness calculated from (8) and (9) are greatly affected by inlet conditions. Figs. 9 and 10 show the changing working air inlet and humidity conditions on WB and dew point effectiveness respectively. For these cases, the working air inlet temperature is varied from 25°C to 45°C and absolute humidity from 8g/kg to 19g/kg keeping the constant air velocity of 1.1m/sec.

It is inferred from these graphs that the effectiveness of HMX increases with increasing working air temperature and decreasing absolute humidity. The increasing air temperature and decreasing moisture content have more tendency of causing evaporation, thus, it can achieve a higher cooling effectiveness.

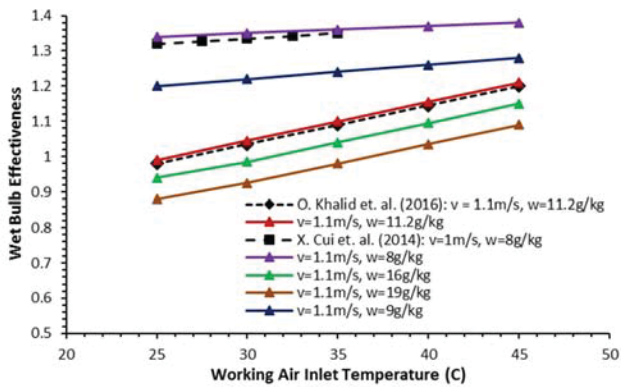


Fig. 9 Working Air Inlet Temperature and Humidity Conditions on WB Effectiveness

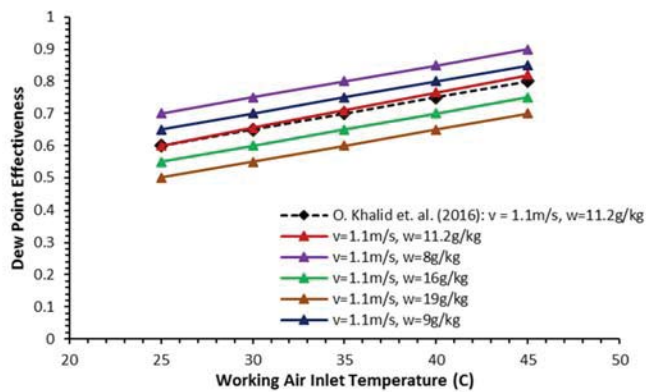


Fig. 10 Working Air Inlet Temperature and Humidity Conditions on Dew Point Effectiveness

At  $45^{\circ}\text{C}$  ( $T_{DBw,f,in}$ ) and  $8\text{g/kg}$  ( $\omega_{w,f}$ ) of inlet conditions of working air the WB and dew point effectiveness can reach as high as 1.3 and 0.88 respectively. X. Cui et al. [10] also deduced the same results as presented in this simulation. These simulated results are also compared with experimental results of O. Khalid [20] both results have shown good compliance.

### C. Effect of Working Air Inlet Velocity on Cooling Effectiveness

As presented in the mathematical model, the Reynolds number, Nusselt number and Sherwood number i.e. (6) – (7) are significantly affected by changing air velocity, thus, affecting heat and mass transfer process. Fig. 11 shows the effect of working air inlet velocity on cooling effectiveness while keeping the preset conditions as mentioned in table I. Velocity changes from 0.3 m/sec to 4 m/sec whereas the effectiveness changes from 0.2 to 1.5.

These results show that higher inlet velocities give lower cooling effectiveness. This is due to the fact that increasing air velocity causes more mass flow rate to enter the HMX, thus decreasing HMX effectiveness to cool the air [15].

X. Cui et al. 2014 [10] suggested to keep the air velocity less than 1.5m/sec for higher cooling effectiveness at a working air inlet temperature of  $30^{\circ}\text{C}$  and  $10\text{g/kg}$  of moisture content. O. Khalid 2016 [20] focused more on lower ranges of velocities

i.e. 0.5 m/sec to 1.1 m/sec and suggested to use air velocity of less than 0.5 m/sec for higher cooling effectiveness. Both of these results can be deduced from this presented model.

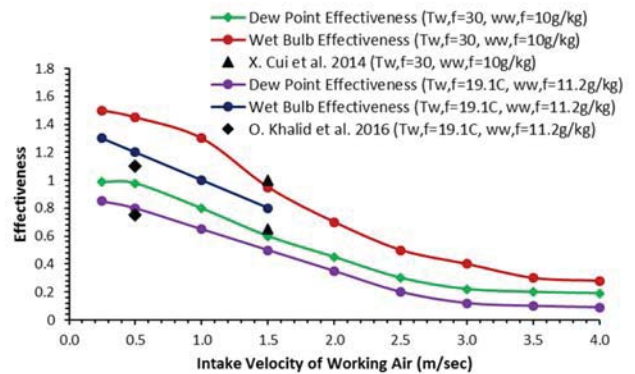


Fig. 11 Inlet air velocity and Effectiveness

### D. Effect of HMX Geometric Parameters on Cooling Effectiveness

Fig. 12 shows the effect of changing product channel height on cooling effectiveness. The simulation is carried by changing product air channel height while keeping the preset conditions. Product air channel height is varied from 3mm to 20mm whereas the WB effectiveness changes from 0.7 to 1.2 and dew point effectiveness changes from 0.5 to 0.8 respectively.

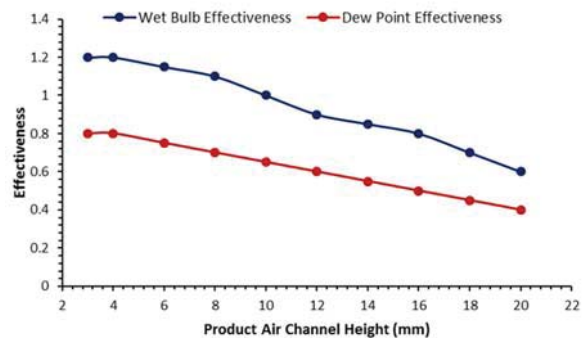


Fig. 12 Product Channel Height and Effectiveness

It is observed that increasing channel height decreases cooling effectiveness. This is due to the fact that increasing the channel height, causes an increase in cross-sectional area, thus offering more product air to come inside the HMX, as a result decreasing the tendency of HMX to handle a bigger mass flow rate. It is suggested to use a lower channel height (less than 5mm) for high cooling effectiveness.

Fig. 13 shows the effect of changing dimensionless channel length (L/H) on cooling effectiveness. Dimensionless channel length is varied from 100 to 450 whereas the WB effectiveness changes from 0.4 to 1.4 and dew point effectiveness changes from 0.2 to 0.8. It is observed that higher L/H ratios gives higher cooling effectiveness. In other words, a longer channel length leads to an increase in the contact time and area, and enhancing heat and mass transfer process. It is recommended to use a channel length of at least 200 [10].

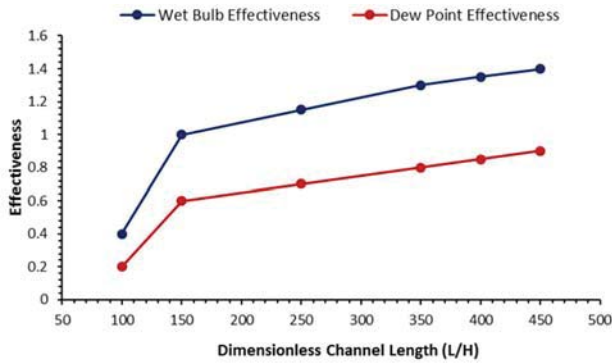


Fig. 13 Dimensionless Channel Length (L/H) and Effectiveness

Fig. 14 shows the effect of changing dimensionless height ratio ( $H_{working}/H_{product}$ ) on cooling effectiveness. The height ratio is varied from 0.3 to 4. The maxima of this curve occur at almost a height ratio of 2. In other words, a maximum cooling effectiveness is achieved for a working air channel height as twice as product air channel height.

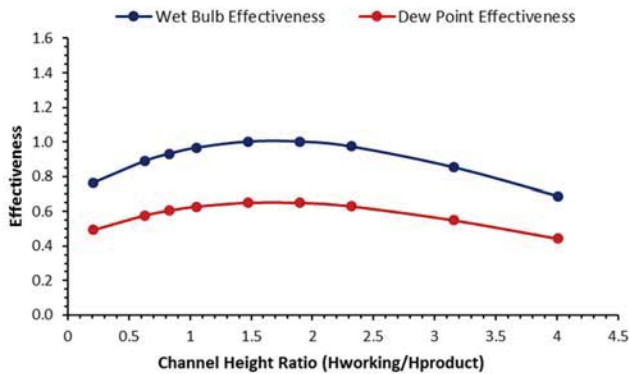


Fig. 14 Channel Height Ratio ( $H_{working}/H_{product}$ ) and Effectiveness

Fig. 15 shows the effect of changing product to working air ratio on cooling effectiveness. This ratio is achieved by changing the cross-sectional area of the channels. This ratio is varied from 0.2 to 3. It is observed that higher values of product to working air ratio leads to a lower value of cooling effectiveness. Since, product air must be supplied to the room so it can't be decreased significantly to achieve higher cooling effectiveness, therefore, at this stage we must do a compromise between flow rate of product air and effectiveness. A good compromise can be that to use a ratio of unity between product air flow rate and working air flow rate. However, a ratio less than unity can be more effective for HMX.

#### E. Effect of Changing Water Temperature on Cooling Effectiveness

Fig. 16 shows the effect of changing water temperature on cooling effectiveness. The water temperature is varied from 18°C to 35°C. It is observed that changing water temperature have no effect on WB or dew point effectiveness.

O. Khalid [20] experimented to see the effect of water on effectiveness for a smaller range of water temperature for common available tap water. This simulated Matlab program

also show a compliance with the experimental results of O. Khalid [20].

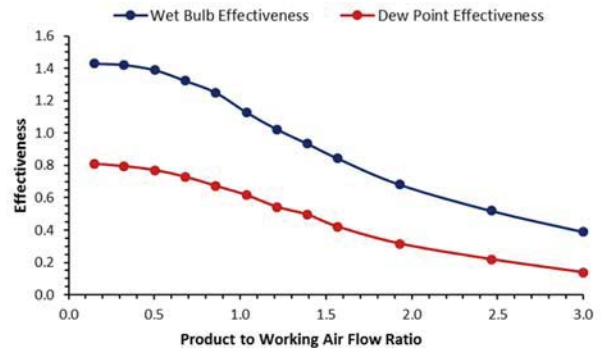


Fig. 15 Product to Working Air Flow Ratio vs Effectiveness

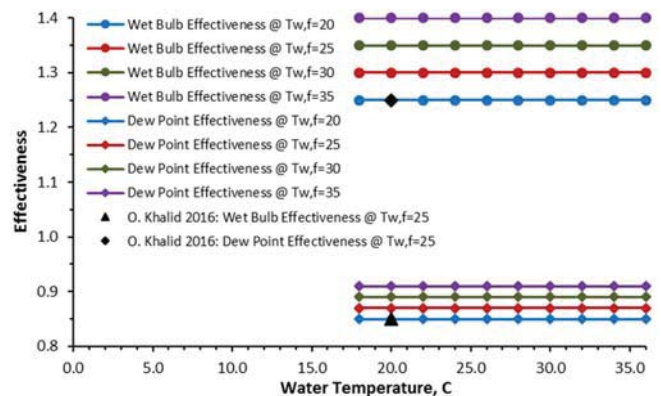


Fig. 16 Effect of Makeup Water Temperature on WB and Dew Point Effectiveness

## VI. CONCLUSION

This study presents theoretical energy analysis of the novel HMX based on M-Cycle used as an IEC in an air conditioning system of a building.

Reasonable assumption is made upon which a mathematical model is established which consists of product air temperature distribution equation, working air temperature distribution, working air humidity distribution and water temperature. Flow regime is defined using Reynolds number, convective heat transfer coefficient is calculated using Nusselt Number, mass transfer coefficient is calculated using Sherwood Number, and the performance measurement parameters like WB effectiveness and dew point effectiveness are defined. A suitable number of elements are selected for convergence criteria. The numerical simulation is validated by a comparison with experimental studies available in the literature.

The simulation is carried for 0.5-ton cooling capacity of product air. The geometric parameters and operational parameters like inlet temperature, humidity, velocities etc are described. The finite difference formulation scheme is adapted for the discretization of governing first order ordinary differential equations. The resulted algebraic equations are solved using Matlab by adapting an iterative methodology.

The simulation results yield the temperature and humidity



plots of working air-dry channel, working air wet channel and product air channel. It was observed that product air is cooled down to a temperature below the WB of working air inlet temperature maintaining a constant absolute humidity.

The HMX cooling performance is analyzed by observing the effect of different geometric properties and operational parameters. It is found that the cooling effectiveness is directly proportional to DB temperature of working air, and inversely proportional with absolute humidity. Cooling performance is high for low inlet velocities, while emphasis is given for air velocities less than 0.5m/sec. Cooling performance is high for a height of channel less than 5mm, however, manufacturing feasibility of 5mm channel height is an important factor, therefore, a channel height of 6-8mm is also recommended for manufacturing ease. It is suggested to use a longer channel length as compared to channel height i.e. length should be 200 times of height, for higher values of effectiveness. Height of working air channel must be kept twice as the height of product air channel. The product to working air ratio must be kept less than unity for high cooling effectiveness. Finally, it is found that changing water temperature have no effect on cooling effectiveness of HMX.

The results presented in this research paper indicate the usefulness of M-Cycle based HMX and allowing to extend the potential of renewable EC.

For future recommendations, it is suggested to work on different flow configurations of water circulation and analyzing the effect of water film thickness on the cooling effectiveness of HMX.

#### REFERENCES

- [1] O. Amer, R. Boukhanouf, and H. G. Ibrahim, "A Review of Evaporative Cooling Technologies," *Interantional J. Environ. Sci. Dev.*, vol. 6, no. 2, pp. 111–117, 2015.
- [2] L. Pérez-Lombard, J. Ortiz, and C. Pout, "A review on buildings energy consumption information," *Energy Build.*, vol. 40, no. 3, pp. 394–398, 2008.
- [3] E. . Machlin, *An Introduction to Aspect of Thermodynamics and Kinetics relevant to Material science*, vol. 1. 2015.
- [4] IEA (International Energy Agency), "Renewables for heating and cooling," *Technology*, pp. 1–210, 2007.
- [5] Y. Jiang and X. Xie, "Theoretical and testing performance of an innovative indirect evaporative chiller," *Sol. Energy*, vol. 84, no. 12, pp. 2041–2055, 2010.
- [6] B. Rianguilaikul and S. Kumar, "An experimental study of a novel dew point evaporative cooling system," *Energy Build.*, vol. 42, no. 5, pp. 637–644, 2010.
- [7] G. L., "Maisotsenko Cycle for Cooling Processes," *Clean Air*, vol. 9, pp. 1–18, 2008.
- [8] H. Caliskan, A. Hepbasli, I. Dincer, and V. Maisotsenko, "Thermodynamic performance assessment of a novel air cooling cycle: Maisotsenko cycle," *Int. J. Refrig.*, vol. 34, no. 4, pp. 980–990, 2011.
- [9] X. Cui, K. J. Chua, M. R. Islam, and W. M. Yang, "Fundamental formulation of a modified LMTD method to study indirect evaporative heat exchangers," *Energy Convers. Manag.*, vol. 88, pp. 372–381, 2014.
- [10] X. Cui, K. J. Chua, and W. M. Yang, "Numerical simulation of a novel energy-efficient dew-point evaporative air cooler," *Appl. Energy*, vol. 136, pp. 979–988, 2014.
- [11] X. Zhao, J. M. Li, and S. B. Riffat, "Numerical study of a novel counter-flow heat and mass exchanger for dew point evaporative cooling," *Appl. Therm. Eng.*, vol. 28, no. 14–15, pp. 1942–1951, 2008.
- [12] G. L. Ding, T. T. Wang, J. D. Gao, Y. X. Zheng, Y. F. Gao, and J. Song, *Developing simulation tools for design of low charge vapour compression refrigeration systems*. Woodhead Publishing Limited, 2013.
- [13] W. Z. Gao, Y. P. Cheng, a. G. Jiang, T. Liu, and K. Anderson, "Experimental investigation on integrated liquid desiccant – Indirect evaporative air cooling system utilizing the Maisotsenko – Cycle," *Appl. Therm. Eng.*, vol. 88, pp. 288–296, 2015.
- [14] S. Anisimov and D. Pandelidis, "Numerical study of the Maisotsenko cycle heat and mass exchanger," *Int. J. Heat Mass Transf.*, vol. 75, pp. 75–96, 2014.
- [15] M. Jradi and S. Riffat, "Experimental and numerical investigation of a dew-point cooling system for thermal comfort in buildings," *Appl. Energy*, vol. 132, pp. 524–535, 2014.
- [16] D. Pandelidis and S. Anisimov, "Numerical analysis of the selected operational and geometrical aspects of the M-cycle heat and mass exchanger," *Energy Build.*, vol. 87, pp. 413–424, 2015.
- [17] S. Anisimov, D. Pandelidis, and J. Danielewicz, "Numerical analysis of selected evaporative exchangers with the Maisotsenko cycle," *Energy Convers. Manag.*, vol. 88, pp. 426–441, 2014.
- [18] D. Pandelidis and S. Anisimov, "Numerical analysis of the heat and mass transfer processes in selected M-Cycle heat exchangers for the dew point evaporative cooling," *Energy Convers. Manag.*, vol. 90, pp. 62–83, 2015.
- [19] S. Anisimov, D. Pandelidis, and V. Maisotsenko, "Numerical study of heat and mass transfer process in the Maisotsenko cycle for indirect evaporative air cooling," *Heat Transf. Eng.*, vol. 7632, no. JANUARY, pp. 1–40, 2016.
- [20] O. Khalid, M. Ali, N. A. Sheikh, H. M. Ali, and M. Shehryar, "Experimental analysis of an improved Maisotsenko cycle design under low velocity conditions," *Appl. Therm. Eng.*, vol. 95, pp. 288–295, 2016.
- [21] C. Zhan, Z. Duan, X. Zhao, S. Smith, H. Jin, and S. Riffat, "Comparative study of the performance of the M-cycle counter-flow and cross-flow heat exchangers for indirect evaporative cooling - Paving the path toward sustainable cooling of buildings," *Energy*, vol. 36, no. 12, pp. 6790–6805, 2011.
- [22] E. N. Sieder and G. E. Tate, "Heat Transfer and Pressure Drop of Liquids in Tubes," *Ind. Eng. Chem.*, vol. 28, pp. 1429–1435, 1936.
- [23] J. R. Welty, C. E. Wicks, R. E. Wilson, and G. L. Rorrer, *Fundamentals of Momentum, Heat, and Mass Transfer*. 2008.
- [24] E. L. Cussler, "Diffusion: Mass Transfer in Fluid Systems," *Engineering*, vol. Second, p. 580, 1997.